INTERNATIONAL JOURNAL FOR NUMERICAL METHODS IN FLUIDS
Int. J. Numer. Meth. Fluids 2008; **56**:401–418
Published online 6 June 2007 in Wiley InterScience (www.interscience.wiley.com). DOI: 10.1002/fld.1528

A higher-order predictor–corrector scheme for two-dimensional advection–diffusion equation

Chuanjian Man[‡] and Christina W. Tsai[*,†,§]

Department of Civil, Structural, and Environmental Engineering, State University of New York at Buffalo, Buffalo, NY 14260, U.S.A.

SUMMARY

A higher-order accurate numerical scheme is developed to solve the two-dimensional advection–diffusion equation in a staggered-grid system. The first-order spatial derivatives are approximated by the fourth-order accurate finite-difference scheme, thus all truncation errors are kept to a smaller order of magnitude than those of the diffusion terms. Therefore, there is no need to add an artificial diffusion term to balance the unwanted numerical diffusion. For the time derivative, the fourth-order accurate Adams–Bashforth predictor–corrector method is applied. The stability analysis of the proposed scheme is carried out using the Von Neumann method. It is shown that the proposed algorithm has good stability. This method also shows much less spurious oscillations than current lower-order accurate numerical schemes. As a result, the proposed numerical scheme can provide more accurate results for long-time simulations. The proposed numerical scheme is validated against available analytical and numerical solutions for one- and two-dimensional transport problems. One- and two-dimensional numerical examples are presented in this paper to demonstrate the accuracy and conservative properties of the proposed algorithm by comparing with other numerical schemes. The proposed method is demonstrated to be a useful and accurate modelling tool for a wide range of transport problems. Copyright © 2007 John Wiley & Sons, Ltd.

Received 1 September 2006; Revised 31 January 2007; Accepted 20 April 2007

KEY WORDS: advection–diffusion equation; staggered grid; predictor–corrector method; high-order numerical schemes

[*]Correspondence to: Christina W. Tsai, 233 Jarvis Hall, Department of Civil, Structural, and Environmental Engineering, State University of New York at Buffalo, Buffalo, NY 14260, U.S.A.
[†]E-mail: ctsai4@eng.buffalo.edu
[‡]Research Assistant.
[§]Assistant Professor.

Contract/grant sponsor: Office of Vice President for Research; contract/grant number: 1036644
Contract/grant sponsor: National Science Foundation; contract/grant number: EAR-0510830

1. INTRODUCTION

Transport of sediments and contaminants has long been one of the great concerns to hydraulic and environmental engineers. Sediment particles in alluvial rivers are subject to random and complex movement. Understanding the transport of sediment particles is of fundamental and practical importance to hydraulic engineering. Accurate simulation of suspended sediment transport is essential for water quality management, environmental impact assessment and design of hydraulic structures. Among others, the advection–diffusion (A–D) equation is crucial to the simulation of suspended sediment transport, solute contaminant transport and water quality in rivers. Therefore, improving the efficiency and accuracy of numerical schemes for the A–D equation has been a focus of research.

Both time and spatial derivatives are presented in the A–D equation. Explicit or implicit time integration schemes for the time derivative can be applied to the A–D equation. Spatial discretization methods for solving the A–D equation can be broadly classified as the finite difference method (FDM), finite volume method, finite element method (FEM) and spectral method [1]. Ii *et al.* [2] presented a finite volume method on triangular meshes for advection transport problems. FEM and FDM are classically used to solve the A–D equation. However, lower-order methods using the advection term often exhibit an oscillatory behaviour or excessive numerical dispersion near relatively sharp concentration fronts [3]. These problems become more serious for advection-dominated transport [4]. Siegel *et al.* [5] developed a numerical scheme based on discontinuous finite elements for the discretization of the advective term and on the mixed approximation of the diffusive term for the solute transport equation in a porous medium. This scheme, however, still introduces a small amount of numerical diffusion when sharp concentration fronts occur. Also, it has increased the computational cost even compared with the high-order finite-difference schemes [5]. FEMs applied to the A–D equation had been concisely reviewed by Franca *et al.* [6] to illustrate the development of numerical schemes for the A–D equation. Compared with FEM, application of the FDM to the A–D equation has gained more popularity, for the FDM is simpler than FEM in general. The classical central-difference approximation of the advection term is simple but suffers from excessive numerical oscillations [7]. Upwind schemes better represent the underlying physics, but an unacceptable degree of numerical diffusion has to be typically introduced [8]. Bruneau *et al.* [9] built a TVD scheme based on a family of second- and third-order Lax–Wendroff-type schemes. Tsai *et al.* [10] proposed a hybrid finite-difference scheme capable of solving pure advection, pure diffusion and dispersion processes by combining two well-known schemes, namely, the Crank–Nicholson second-order central-difference scheme and the Crank–Nicholson Galerkin FEM with linear basis functions. There are still continuing interests in solving the one- or two-dimensional A–D equation by the FDM [11, 12]. All these studies attempted to decrease the commonly seen excessive artificial diffusion and spurious oscillations introduced by the numerical method. However, the above-mentioned schemes used lower-order accurate time-stepping methods for the A–D equation and therefore have lower accuracy of numerical solutions for a fixed time step.

For time-stepping methods, explicit schemes have the virtue of computational efficiency and simplicity. An explicit scheme of growing popularity in free-surface codes is the QUICKEST method [13]. This scheme can be considered to be central differencing plus a higher-order upwind-biased correction to cancel the third-order Taylor-series error. When used with the explicit Euler time advancement, QUICK (e.g. [14, 15]) is not stable for pure advection problems [16]. Implicit methods are generally more stable, but require iterative methods and thus are costly and time

DOI: 10.1002/fld

consuming [17]. The predictor–corrector method attempts to combine best of both explicit and implicit methods. The efficiency, accuracy and good stability properties of the Adams–Bashforth predictor–corrector method have been demonstrated for wave equations [18, 19].

In this study, we develop a new finite-difference numerical scheme for the A–D equation in a staggered-grid system. One of the important advantages of the staggered-grid scheme is the good conservation property of the mass (e.g. [18, 20]). In addition, Orszag pointed out that the staggered-mesh scheme is usually more accurate than non-staggered-grid scheme [21]. In this paper, the fourth-order Adams–Bashforth predictor–corrector scheme is employed for time stepping and the fourth-order accurate central finite-difference scheme for the first-order spatial derivatives. The stability analysis will be carried out using the Von Neumann method. The accuracy of the proposed model will be investigated in the examples of both one- and two-dimensional A–D problems. In these examples, the numerical results are compared to available theoretical and/or numerical results.

2. GOVERNING EQUATION

The aim of this work is to construct a higher-order efficient numerical scheme for the two-dimensional A–D equation in the conservative form

$$\frac{\partial C}{\partial t}+\frac{\partial (UC)}{\partial x}+\frac{\partial (VC)}{\partial y}=\frac{\partial}{\partial x}\left(D_x\frac{\partial C}{\partial x}\right)+\frac{\partial}{\partial y}\left(D_y\frac{\partial C}{\partial y}\right) \tag{1}$$

where C is the suspended load concentration, U and V are the depth-averaged horizontal fluid velocity components in the x- and y-direction, respectively; D_x and D_y are diffusion coefficients in the x- and y-direction, respectively. The main difficulty in solving this equation comes from the advection term because numerical oscillations in the solution appear when an improper scheme is applied [22]. We develop a fourth-order finite-difference numerical scheme for the advection terms in a staggered-grid system to overcome this problem in this paper. The fourth-order Adams predictor–corrector scheme is used to approximate the time derivative term. The predictor–corrector method consists of a predictor step and a corrector step in each interval. The predictor estimates the solution for a new point, and then the corrector improves the accuracy of the solution. The predictor–corrector method uses the information from previous points instead of the intermediate points in each interval. Figure 1 shows the schematic of the predictor–corrector method.

To apply the predictor–corrector method to Equation (1), we define a new function E, which involves spatial derivatives of C and (U, V) as follows:

$$E(C,U,V)=-\frac{\partial (CU)}{\partial x}-\frac{\partial (CV)}{\partial y}+\frac{\partial}{\partial x}\left(D_x\frac{\partial C}{\partial x}\right)+\frac{\partial}{\partial y}\left(D_y\frac{\partial C}{\partial y}\right) \tag{2}$$

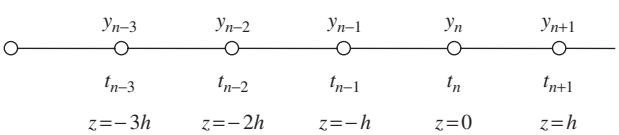

Figure 1. Grid points used in the predictor–corrector method.

DOI: 10.1002/fld

Now, rewrite Equation (1) as

$$\frac{\partial C}{\partial t} = E(C, U, V) \tag{3}$$

3. NUMERICAL MODEL

3.1. Mesh discretization and variable definition

In this study, a staggered-grid system will be used in the numerical discretization of spatial derivatives. Figure 2 illustrates this staggered-grid system in which all scalars such as concentration C and water depth h are defined at the cell centre, while vectors such as velocity components U and V are defined at the interfaces of the cell. The meshes are numbered by $i = 1, 2, \ldots, m$ in the x-direction and $j = 1, 2, \ldots, n$ in the y-direction. m and n are the total number of grid points in the x- and y-direction, respectively. The mesh sizes in the x- and y-direction are represented by Δx and Δy, respectively. And the time step is represented by Δt. The vectors at centre of the cell are obtained by the linear interpolation. For example, the fluid velocity at the centre of the cell $U_{i,j}$ can be obtained as follows:

$$U_{ij} = \tfrac{1}{2}(U_{i-1/2,j} + U_{i+1/2,j}) \tag{4}$$

3.2. Time matching by fourth-order predictor–corrector method

The governing equation (3) is marched in time by the fourth-order accurate Adams predictor–corrector method in which the time level n refers to the present time with all information known. First, the predictor step is implemented to Equation (3) by the explicit third-order Adams–Bashforth scheme (e.g. [23, 24]):

$$C_{i,j}^{n+1} = C_{i,j}^{n} + \frac{\Delta t}{12}[23E_{i,j}^{n} - 16E_{i,j}^{n-1} + 5E_{i,j}^{n-2}] \tag{5}$$

where all information on the right-hand side of the equation is known from previous calculations. The values of $C_{i,j}^{n+1}$ are thus straightforward to obtain.

After the predictor step, the predicted values, $C_{i,j}^{n+1}$, are known. We can thus obtain the corresponding values of E based on Equation (2). This information can be applied in the corrector step

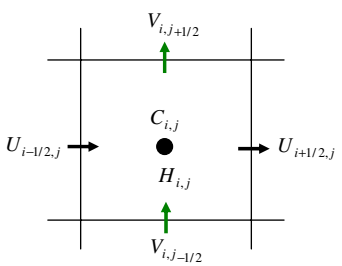

Figure 2. The staggered-grid system used in the two-dimensional model.

DOI: 10.1002/fld

using the fourth-order Adams–Moulton method:

$$C_{i,j}^{n+1} = C_{i,j}^{n} + \frac{\Delta t}{12}[9E_{i,j}^{n+1} + 19E_{i,j}^{n} - 5E_{i,j}^{n-1} + E_{i,j}^{n-2}] \tag{6}$$

The predictor–corrector procedure is repeated until the error between two successive results reaches a required limit. The numerical error, $\Delta\overline{C}$, will be computed for the variable as defined in Equation (7)

$$\Delta\overline{C} = \frac{\sum_{i,j} |C_{i,j}^{n+1} - C_{i,j}^{(n+1)*}|}{\sum_{i,j} |C_{i,j}^{n+1}} \tag{7}$$

In this study, the stopping criterion of the iteration is $\Delta\bar{C} < 0.001$ and the number of iterations in the numerical experiments is usually less than three.

3.3. Finite-difference approximation for spatial derivatives

The first-order derivatives of advective flux $f = UC$, in x-direction in the domain except near the boundary (i.e. $i = 3, 4, \ldots, m-2$) are discretized by the fourth-order accurate four-point central-difference method. Therefore, the leading order truncation error is within the fifth order of magnitude. All the lower-order terms, the second-, the third- and the fourth-order errors, are eliminated. Thus, all truncation errors are kept to a smaller order of magnitude compared to the second-order diffusion terms. For example,

$$\left(\frac{\partial f}{\partial x}\right)_{i,j} = \frac{f_{i-2,j} - 8f_{i-1,j} + 8f_{i+1,j} - f_{i+2,j}}{12\Delta x} - \frac{1}{30}\frac{\partial^5 f}{\partial x^5}\Delta x^4 \quad (i = 3, 4, \ldots, m-2) \tag{8}$$

The first-order derivatives near the boundary (i.e. $i = 2, m-1$) are discretized by the five-point finite-difference scheme. For example,

$$\left(\frac{\partial f}{\partial x}\right)_{2,j} = \frac{-3f_{1,j} - 10f_{2,j} + 18f_{3,j} - 6f_{4,j} + f_{5,j}}{12\Delta x} \tag{9}$$

$$\left(\frac{\partial f}{\partial x}\right)_{m-1,j} = \frac{3f_{m-1,j} + 10f_{m-2,j} - 18f_{m-3,j} + 6f_{m-4,j} - f_{m-5,j}}{12\Delta x} \tag{10}$$

The second-order derivative of concentration in the domain except near the boundary is discretized by the three-point central-difference method. For example,

$$\left(\frac{\partial^2 C}{\partial x^2}\right)_{i,j} = \frac{1}{\Delta x^2}(C_{i-1,j} - 2C_{i,j} + C_{i+1,j}) + \frac{1}{12}\frac{\partial^4 C}{\partial x^4}\Delta x^2 \quad (i = 2, 3, \ldots, m-1) \tag{11}$$

The second-order derivative of concentration is discretized by the four-point forward and backward FDM at the right and left-hand side boundaries, respectively. For example,

$$\left(\frac{\partial^2 C}{\partial x^2}\right)_{1,j} = \frac{1}{\Delta x^2}(2C_{1,j} - 5C_{2,j} + 4C_{3,j} - C_{4,j}) \tag{12}$$

DOI: 10.1002/fld

A similar expression in the y-direction can be obtained for both the first-order and second-order derivatives. From Equations (8) and (11), we can find that errors associated with the third-order derivatives have been eliminated.

For the one-dimensional A–D equation, based on LeVeque [25], a FDM is considered conservative if it can be expressed as

$$C_i^{n+1} = C_i^n - \frac{\Delta t}{\Delta x}[\mathrm{FLUX}(C_{i-p}^n, C_{i-p+1}^n, \ldots, C_{i+q}^n) - \mathrm{FLUX}(C_{i-p-1}^n, C_{i-p}^n, \ldots, C_{i+q-1}^n)] \quad (13)$$

where FLUX is the sum of advective flux and diffusive flux. On the other hand, similar definitions can be found and expressed as [26]

$$\sum_i C_i^{n+1} \Delta x = \sum_i C_i^n \Delta x \quad (14)$$

The present numerical scheme can be proved as conservative in the computational domain except at the boundaries based on either Equation (13) or (14) (e.g. combine Equations (5), (8) and (11) for the predictor step; combine Equations (6), (8) and (11) for the corrector step).

4. STABILITY ANALYSIS

A Von Neumann stability analysis is applied to analyse the stability of the present numerical scheme. For a uniform flow and a constant diffusion coefficient, Equation (1) in the x-direction can be re-written as

$$\frac{\partial C}{\partial t} = -U\frac{\partial C}{\partial x} + D\frac{\partial}{\partial x}\left(\frac{\partial C}{\partial x}\right) \quad (15)$$

The corresponding E becomes

$$E(C, U) = -U\frac{\partial C}{\partial x} + D\frac{\partial^2 C}{\partial x^2} \quad (16)$$

We denote that

$$C_i^n = C_0 G^n \exp(I\mathrm{i}\theta) \quad (17)$$

where $I = \sqrt{-1}$ is the imaginary unit, $\theta = 2\pi\Delta x/L$ is the phase angle, C_0 is the initial concentration of the problem, and G is the amplification factor. Substituting the above definition into the Adams–Bashforth *predictor* method, Equation (5), we obtain

$$G^2(G-1) - \beta_1(23G^2 - 16G + 5) = 0 \quad (18)$$

where

$$\beta_1 = \frac{U \cdot \Delta t}{\Delta x}\left[\frac{-8\sin(\theta) + \sin(2\theta)}{12 \times 6}\right] I + \frac{1}{6}\frac{\Delta t \cdot D}{(\Delta x)^2}(\cos(\theta) - 1) \quad (19)$$

Equation (18) can be solved for $|G|$ as a function of θ, given a constant dispersion number and Courant number. The dispersion number, γ, has the form

$$\gamma = \frac{\Delta t \cdot D}{(\Delta x)^2} \quad (20)$$

DOI: 10.1002/fld

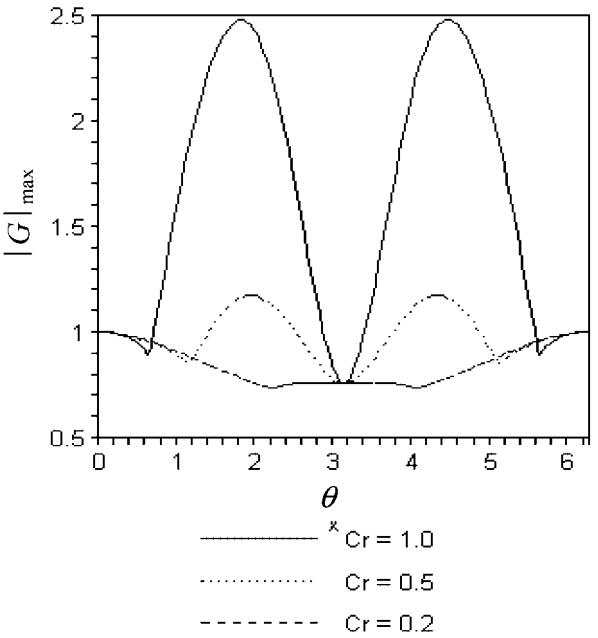

Figure 3. The maximum modulus of the amplification factor $|G|_{\max}$ as a function of the phase angle θ for the predictor scheme, $Cr = \{1.0, 0.5, 0.2\}$.

And the Courant number, Cr, is

$$Cr = U\left(\frac{\Delta t}{\Delta x}\right) \tag{21}$$

With the definition of dispersion number and Courant number, Equation (19) becomes

$$\beta_1 = Cr\left[\frac{-8\sin(\theta) + \sin(2\theta)}{72}\right] I + \frac{\gamma}{6}(\cos(\theta) - 1) \tag{22}$$

There are three variables, Courant number, dispersion number and phase angle, in Equation (18). By selecting three representative Courant numbers ($Cr = \{0.2, 0.5, 1.0\}$) and $\gamma = 0.4$, we can plot the maximum modulus of the amplification factor as shown in Figure 3. It is found that the predictor scheme is stable when the Courant number is smaller than 0.5 and the dispersion number is less than 0.5.

Similarly, the stability of the fourth-order Adams–Moulton *corrector* method, Equation (6), can be investigated. The stability of the corrector scheme can be determined by the following equation:

$$G^2(G-1) - \beta_2(9G^3 + 19G^2 - 5G + 1) = 0 \tag{23}$$

where

$$\beta_2 = Cr\left[\frac{-8\sin(\theta) + \sin(2\theta)}{24 \times 6}\right] I + \frac{\gamma}{12}(\cos(\theta) - 1) \tag{24}$$

DOI: 10.1002/fld

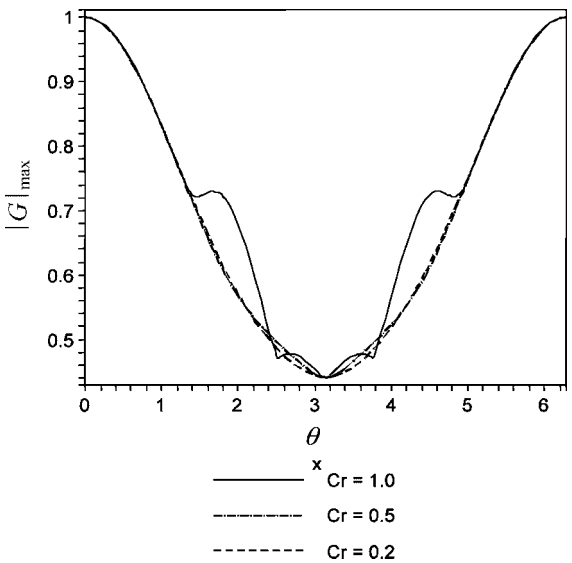

Figure 4. The maximum modulus of the amplification factor $|G|_{\max}$ as a function of the phase angle θ for the corrector scheme, $Cr = \{1.0, 0.5, 0.2\}$.

Figure 4 shows the maximum modulus of the amplification factor as a function of the phase angle by selecting three representative values ($Cr = \{0.2, 0.5, 1.0\}$) and $\gamma = 0.4$. The corrector scheme is stable when Cr is smaller than or equal to 1.0. Considering the combined effect of dispersion and advection, the Courant number and dispersion number obtained above usually range from 0.1 to 0.5 for two-dimensional problems in proposed numerical experiments of this paper.

5. NUMERICAL RESULTS

In the following section, we shall present a series of numerical experiments including advection and advection–diffusion transport problems. Special attention will be paid to avoid the artificial diffusion and spurious oscillations in the present model, which are essential for the accurate simulation of transport processes. Both one- and two-dimensional transport problems will be presented. Six numerical examples will be presented to investigate the computational performance of the proposed scheme: (i) pure advection of both the Gaussian and trapezoidal concentration distributions in one-dimensional uniform flow; (ii) dispersion of a Gaussian concentration distribution in one-dimensional uniform flow; (iii) one-dimensional viscous Burgers equation; (iv) pure advection of a Gaussian concentration distribution in two-dimensional uniform flow; (v) pure advection of a Gaussian concentration distribution in two-dimensional rigid-body rotating flow; and (vi) advection and diffusion of a Gaussian concentration distribution in two-dimensional rigid-body rotating flow.

5.1. One-dimensional examples

5.1.1. Pure advection in uniform flow. Pure advection of both the Gaussian and trapezoidal concentration distributions in one-dimensional uniform flow will be presented in this example. First,

DOI: 10.1002/fld

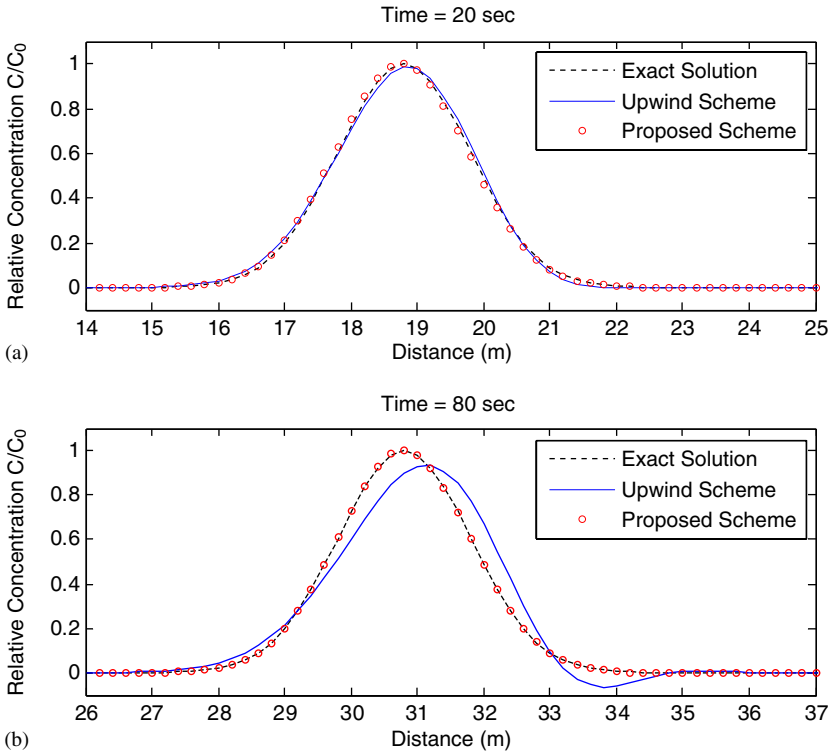

Figure 5. Comparison of analytical solution and numerical solutions by proposed scheme and upwind scheme for 1D pure advection of Gaussian concentration distribution, $U = 0.2\,\text{m/s}$, $\Delta t = 0.2\,\text{s}$, $\Delta x = 0.2\,\text{m}$.

an initial concentration of a Gaussian distribution is advected with a uniform velocity $U = 0.2\,\text{m/s}$. A grid space of 0.2 m and a time interval of 0.2 s are applied in this example. The Courant number in this numerical experiment is 0.2. The renowned upwind scheme is also applied here as an example to solve the same problem. This scheme is often considered to be efficient and simple for simulating smooth concentrations. Figure 5 shows that the numerical solution by the proposed method is almost identical to the analytical solution, without any phase errors presented. The solution by the upwind scheme agrees with the exact solution well at the beginning stage in Figure 5(a). For longer-time simulations, discrepancy between the upwind scheme and exact solution becomes more apparent. Furthermore, there are no numerical oscillations of the proposed scheme, shown in Figure 5, compared with others that present numerical oscillations (e.g. [10, 15]). In addition, there is no mass loss even after a longer-time simulation by the proposed scheme. The numerical experiment is run on a dell Precision 450 workstation. The computer time by the upwind scheme is about 0.255 s for 800 time steps, whereas the computer time is 0.262 s by the proposed scheme. For this example, the computer time by the proposed scheme is about 3% more than the upwind scheme. Secondly, an initial concentration of a trapezoidal distribution is advected with a uniform velocity $U = 1\,\text{m/s}$. A grid space of 100 m and a time interval of 50 s are applied in this example. The Courant number in this numerical experiment is 0.5. We can conclude from

DOI: 10.1002/fld

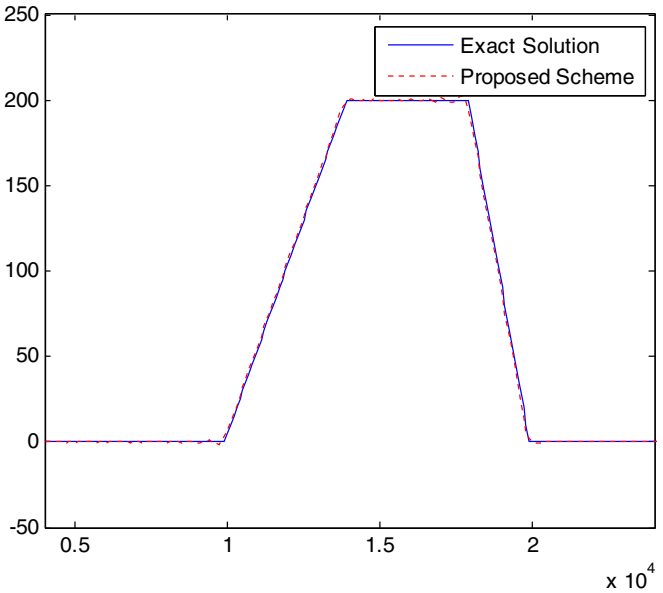

Figure 6. Comparison of exact and numerical solutions for trapezoidal distribution, ($t = 4000$ s), $U = 1.0$ m/s, $\Delta t = 50$ s, $\Delta x = 100$ m.

Figure 6 that the numerical solution by the proposed scheme agrees well with the exact solution. The good mass conservative property of the proposed staggered-grid scheme has been shown in these two examples. It is also demonstrated that the proposed scheme is more accurate than upwind scheme.

5.1.2. Advection and diffusion in uniform flow. The diffusion of a Gaussian concentration distribution with a uniform velocity $U = 0.5$ m/s and a dispersion coefficient $D = 0.2$ m^2/s is simulated. The grid space is 0.5 m and time step is 0.3 s, and the corresponding Courant number and dispersion number are 0.3 and 0.24, respectively. The analytical solution given by the Gaussian probability density function is

$$C(x,t) = \frac{M}{2\sqrt{\pi D t}} \exp\left[-\frac{1}{4Dt}(x - Ut)^2\right] = \frac{1}{\sqrt{0.4t}} \exp\left[-\frac{1}{0.8t}(x - 0.5t)^2\right] \tag{25}$$

where $M = \sqrt{2\pi}$. Both the numerical solution and the analytical solution are drawn in Figure 7. From Figure 7, the numerical solution is almost identical to the analytical solution and there are no numerical diffusion and oscillations presented. The example also shows that the proposed higher-order accurate scheme does not need stricter stability conditions and has a good mass conservative property.

5.1.3. Calculation of viscous Burgers equation. To further investigate the capability of the proposed scheme for solving non-linear problems, a viscous Burgers equation is considered. The

DOI: 10.1002/fld

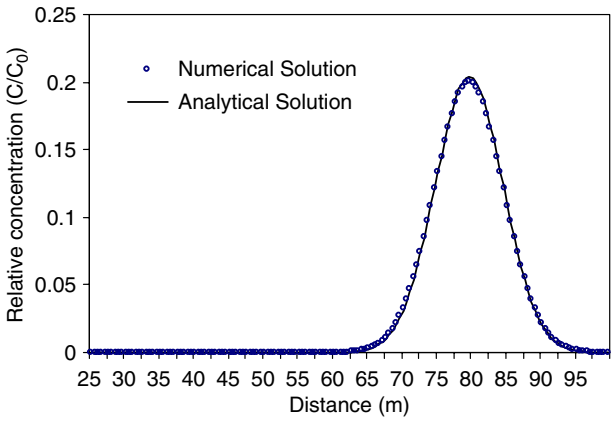

Figure 7. Comparison of numerical solution and analytical solution for one-dimensional advection dispersion of Gaussian concentration distribution ($t = 150\,\text{s}$), $U = 0.5\,\text{m/s}$, $D = 0.2\,\text{m}^2/\text{s}$, $\Delta t = 0.3\,\text{s}$, $\Delta x = 0.5\,\text{m}$.

viscous Burgers equation can be expressed as

$$\frac{\partial C}{\partial t} + \frac{1}{2}\frac{\partial (C^2)}{\partial x} = D\frac{\partial}{\partial x}\left(\frac{\partial C}{\partial x}\right) \tag{26}$$

There exist different solutions given different initial and boundary conditions [27].

With the initial and boundary conditions

$$C(x,0) = 1, \quad x \leqslant 0$$

$$C(x,0) = 0, \quad x > 0$$

$$C(-\infty, t) = 1, \quad C(\infty, 0) = 0, \quad t > 0 \tag{27}$$

The exact solution of the above problem is (e.g. [26])

$$C(x,t) = \left\{1 + \exp\left[\frac{1}{2D}\left(x - \frac{1}{2}t\right)\right]\frac{\operatorname{erfc}(-x/2\sqrt{Dt})}{\operatorname{erfc}[(x-t)/2\sqrt{Dt}]}\right\}^{-1} \tag{28}$$

where erfc is the complementary error function. The numerical solution of the proposed scheme at time $t = 4\,\text{s}$ is depicted in Figure 8 with a grid space of 0.02 m, a time step of 0.01 s and the diffusion coefficient of $0.02\,\text{m}^2/\text{s}$. The range of Courant number used in this example is from 0 to 0.5, whereas the dispersion number is treated as constant, 0.5. Figure 8 shows that the result obtained by the proposed scheme agrees very well with the exact solution. This numerical example demonstrates that the proposed scheme can be accurately applied to the non-linear problem too.

DOI: 10.1002/fld

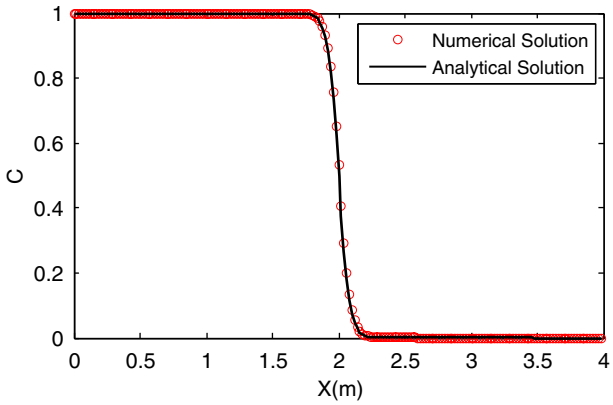

Figure 8. Computational results of one-dimensional viscous Burgers equation by the proposed scheme.

5.2. *Two-dimensional examples*

5.2.1. Pure advection in uniform flow. This example is a typical example to test the advection property (e.g. [12, 18]). To compare the current scheme with other numerical schemes, here the same flow conditions used in Tsai's scheme [28] will be applied. A Gaussian concentration distribution has an initial peak value of 10 ppm and $\sigma_x = \sigma_y = 220$ m. The flow has a constant velocity $U = 0.5$ m/s and $V = 0.5$ m/s in a two-dimensional infinite domain. The initial central position of this Gaussian distribution is at $(x, y) = (1500, 1500\,\text{m})$. A grid size of 100 m × 100 m and a time step of 100 s are used for the simulation. The Courant number for this example is 0.5. Figure 9 shows the bird's eye view of the computed results after 10 000 s. Table I displays the maximum and minimum values of the proposed scheme and other several numerical schemes [14, 28–30]. Compared with other schemes, the proposed scheme has the closest values to the exact solution for both maximum and minimum values without resorting to a finer time step or spatial grid. The proposed scheme is shown to have good mass conservative properties and higher-order accuracy.

5.2.2. Pure advection in rigid-body rotating flow. A numerical example of pure advection of a Gaussian concentration distribution in a two-dimensional rigid-body rotating flow is adopted to investigate the application of the proposed scheme to the flow field with non-uniform flow velocity. The square domain is discretized into a uniform mesh of 100 × 100 grids with $\Delta x = \Delta y = 50$ m. The steady flow field rotates as a solid body about its centre at an angular velocity of 0.314 rad/h, yielding a range of fluid velocity from 0 at the domain centre to 0.31 m/s at the domain edges. The initial Gaussian pulse at $t = 0$ is located at the midpoint of the positive x-axis and the origin of y-axis and $\sigma_x = \sigma_y = 220$ m. This problem was run for three full rotations (60 h) compared with other studies (e.g. [10, 12, 16, 31]) with only one full rotation. With a time step of 40 s, the range of Courant numbers used in the x- and y-direction is from 0 to 0.25. Figure 10 shows the bird's eye view of the computed results after 60 h. The maximum and minimum values of simulated results by the proposed scheme for three turns, the ADI-QUICK scheme and the ADI-TCSD scheme after one turn of rotation are shown in Table II. The results agree well with the exact solution,

DOI: 10.1002/fld

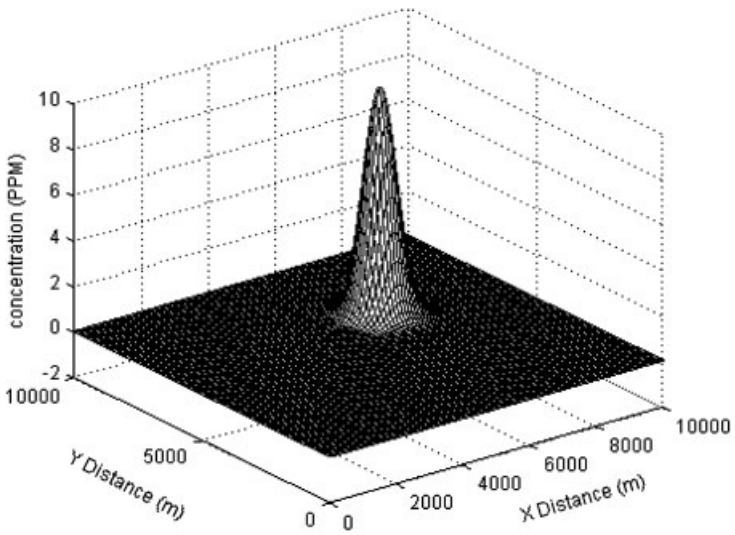

Figure 9. Bird's eye view of computed results for two-dimensional pure advection of Gaussian concentration distribution ($t = 10\,000$ s), $\Delta x = \Delta y = 100$ m.

Table I. Maximum and minimum values for two-dimensional pure advection in uniform flow.

Scheme	Maximum	Minimum
Exact solution	10	0.000
Proposed	9.91	−0.002
Tsai *et al.**	9.87	−0.010
Holly-Preissmann*	9.60	−0.008
ADI-QUICK*	6.96	−0.957
MOSQUITO*	6.62	−0.959

*Values from Tsai *et al.* [28].

and it is found that the error in the peak concentration is less than 1%. It is obvious that the proposed scheme has a better solution in this numerical example for both maximum and minimum values of the concentration. From this example, it is evidently shown that the proposed numerical scheme is also suitable to accurately solve the two-dimensional advection problem with a varying flow velocity field. The proposed scheme built in a staggered-grid system is demonstrated to have higher-order accuracy even after three full rotations in this example.

5.2.3. Advection–diffusion in rigid-body rotating flow. A standard test problem, related to recirculating flows, is the advection and diffusion of a Gaussian pulse in a rotating flow field. This numerical example provides an example to validate the numerical scheme for a two-dimensional advection–dispersion equation with a varying velocity field and an established analytical solution.

DOI: 10.1002/fld

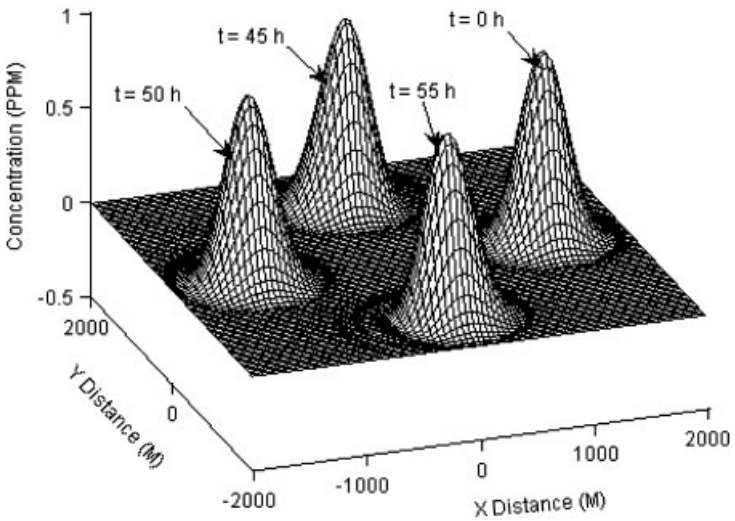

Figure 10. Bird's eye view of pure advection of Gaussian pulse in solid body rotation field $\omega = 0.314\,\text{rad/h}$, $\Delta t = 40\,\text{s}$, $\Delta x = \Delta y = 50\,\text{m}$.

Table II. Maximum and minimum values for two-dimensional pure advection in rotation flow.

Scheme	Maximum (%)	Minimum (%)
Exact solution	100	0.00
Proposed	99.1	−0.02
Proposed (after three rotation)	97.3	−0.4
Tsai *et al.**	97.8	−0.2
ADI-QUICK*	66.3	−5.7
ADI-TCSD*	64.6	−1.8

*Values from Tsai *et al.* [10].

Moreover, this example has been used widely to test different numerical schemes, such as numerical stability and numerical diffusion, spurious oscillations and phase errors (e.g. [12, 16, 28, 31–34]). Furthermore, in this example, the transport changes from the advection dominance near the boundary of the domain to the diffusion dominance in the region close to the centre. The above-mentioned issues often arise in many important applications, which are more difficult to simulate compared with purely advection-dominated problems [34].

In this example, the initial condition $c_0(x, y)$ is given as

$$c_0(x, y) = \exp\left[-\frac{(x - x_c)^2 + (y - y_c)^2}{2\sigma^2}\right] \tag{29}$$

DOI: 10.1002/fld

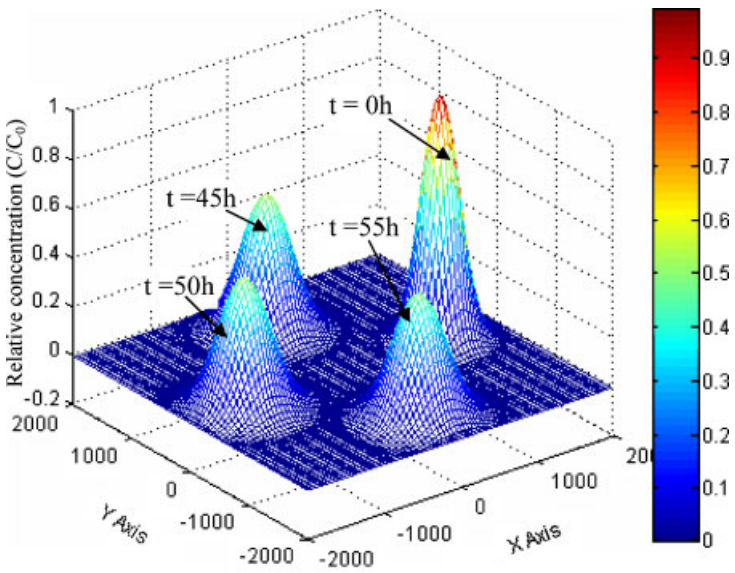

Figure 11. Bird's eye view of the advection–diffusion of Gaussian pulse in solid body rotation field $\omega = 0.314\,\text{rad/h}$, $\Delta t = 40\,\text{s}$, $\Delta x = \Delta y = 50\,\text{m}$, $D_x = D_y = 0.1\,\text{m}^2/\text{s}$.

where (x_c, y_c) and σ are the centre position and standard deviation, respectively. $c_0(x, y)$ is centred at (x_c, y_c) with a minimum value of 0 and a maximum value of 1 and $\sigma = 200\,\text{m}$. The corresponding analytical solution for this problem, with a constant diffusion coefficient D, is given by [34]

$$c(x, y, t) = \frac{2\sigma^2}{2\sigma^2 + 4Dt} \exp\left[-\frac{(\bar{x} - x_c)^2 + (\bar{y} - y_c)^2}{2\sigma^2 + 4Dt}\right] \tag{30}$$

where $\bar{x} = x\cos(\omega t) + y\sin(\omega t)$ and $\bar{y} = -x\sin(\omega t) + y\cos(\omega t)$ and ω is the angular velocity. The square domain is discretized into a uniform mesh of 100×100 grids with $\Delta x = \Delta y = 50\,\text{m}$. The steady flow field rotates as a solid body about its centre at an angular velocity $\omega = 0.314\,\text{rad/h}$, yielding a range of fluid velocity from 0 at the domain centre to 0.31 m/s at the domain edge. The diffusion coefficients are $D_x = D_y = 0.1\,\text{m}^2/\text{s}$. With a time step of 40 s, the range of Courant numbers used in the x- and y-direction is from 0 to 0.25. The program is also run on a dell Precision 450 workstation. The computer time for 5000 time steps is about 45 s. Figure 11 shows the bird's eye view of the computed results after two rotations. The computed results in a cross section of the pulse, together with the analytical solution, are shown in Figure 12. It can be seen that the proposed method has very good accuracy, for the numerical solution agrees with the analytical solution very well even after two rotations. Figure 13 presents the contour of concentrations after two rotations. It can be shown that the discrepancy of the numerical solution and analytical solution is very limited. From the numerical results, we find that the spurious oscillations and phase errors are very limited for such a complex problem by the proposed higher-order accurate scheme presented in this paper.

DOI: 10.1002/fld

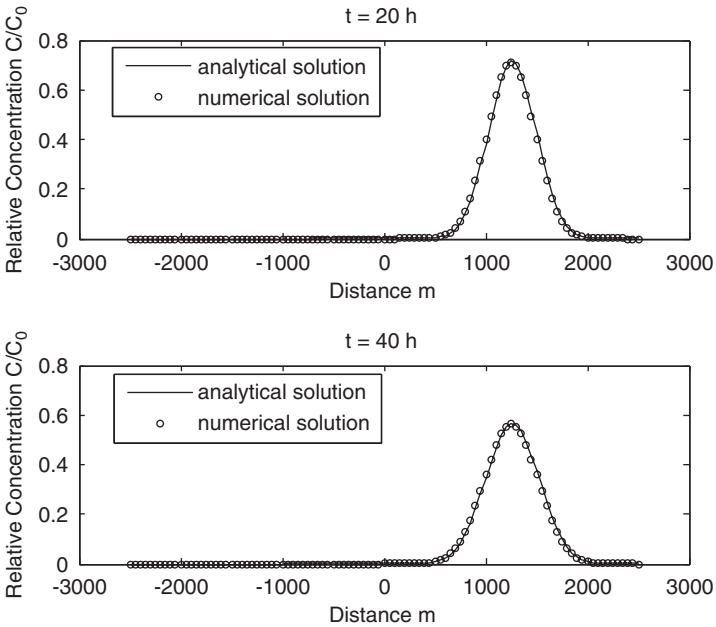

Figure 12. Profile of normalized concentration of advection–diffusion of Gaussian pulse in circular flows. $\omega = 0.314\,\text{rad/h}$, $\Delta t = 40\,\text{s}$, $\Delta x = \Delta y = 50\,\text{m}$, $D_x = D_y = 0.1\,\text{m}^2/\text{s}$.

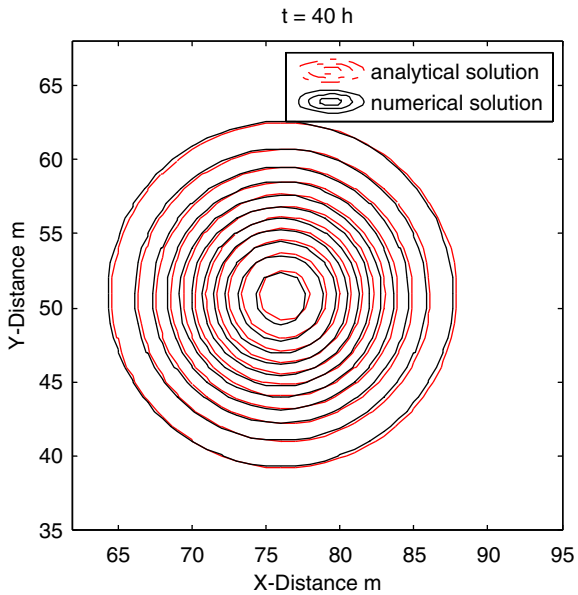

Figure 13. Concentration contour plot of advection–diffusion of Gaussian pulse in circular flows, $\omega = 0.314\,\text{rad/h}$, $\Delta t = 40\,\text{s}$, $\Delta x = \Delta y = 50\,\text{m}$, $D_x = D_y = 0.1\,\text{m}^2/\text{s}$.

DOI: 10.1002/fld

6. CONCLUSIONS

In this study, a fourth-order accurate predictor–corrector algorithm has been developed for solving the advection–diffusion equation in a staggered-grid system. It is demonstrated that the proposed numerical model without an artificial numerical diffusion term has very good numerical convergence. The leading order truncation error of the convection term is kept within a higher order of magnitude, thus resulting in a higher order of accuracy and very limited numerical diffusion. The proposed scheme has reduced significantly both the numerical diffusion and spurious oscillations. The stability of the proposed scheme has been investigated by the Von Neumann method. It is shown that there is no stricter stability requirement for this higher-order explicit numerical scheme even with a combined effect of diffusion and advection. The model is verified by several one- and two-dimensional pure advection and advection–diffusion examples. The numerical results are compared with analytical solutions and by other numerical methods. The comprehensive testing examples have demonstrated that the proposed scheme has much better accuracy and less spurious oscillations. Furthermore, there is no need to add anti-diffusion terms to the proposed scheme to balance the unwanted numerical diffusion. The example of a Gaussian pulse in a rotating field also shows that the proposed model can be applied to accurately simulating complex transport processes. The good conservative properties of the proposed scheme have also been shown in the proposed examples. There is a potential for the proposed scheme to be coupled with a hydrodynamic model to simulate the practical transport process in the complex flow velocity field.

ACKNOWLEDGEMENTS

The writers gratefully acknowledge the financial support from the Office of Vice President for Research at SUNY at Buffalo through the IRCAF Award no. 28466 Project no. 1036644. This work is also partially supported by the National Science Foundation under Grant contract number EAR-0510830.

REFERENCES

1. Akella S, Navon IM. A comparative study of the performance of high resolution advection schemes in the context of data assimilation. *International Journal for Numerical Methods in Fluids* 2006; **51**:719–748.
2. Ii S, Shimuta M, Xiao F. A 4th-order and single-cell-based advection scheme on unstructured grids using multi-moments. *Computer Physics Communications* 2005; **173**:17–33.
3. Huyakorn PS, Pinder GF. *Computational Methods in Subsurface Flow*. Academic Press: London, U.K., 1983.
4. Diaw EB, Lehmann F, Ackerer Ph. One-dimensional simulation of solute transfer in saturated–unsaturated porous media using the discontinuous finite elements method. *Journal of Contaminant Hydrology* 2001; **51**:197–213.
5. Siegel P, Mose R, Ackerer PH, Jaffre J. Solution of advection–diffusion equation using a combination of discontinuous and mixed finite elements. *International Journal for Numerical Methods in Fluids* 1997; **24**: 595–613.
6. Franca LP, Hauke G, Masud A. Revisiting stabilized finite element methods for the advective–diffusive equation. *Computer Methods in Applied Mechanics and Engineering* 2006; **195**:1560–1572.
7. Neuman SP. An Eulerian–Lagrangian scheme for the dispersion–convection equation using conjugate space–time grids. *Journal of Computational Physics* 1981; **41**:270–294.
8. Holly Jr FM, Usseglio-Polatera J. Dispersion simulation in two-dimensional tidal flows. *Journal of Hydraulic Engineering* 1984; **110**(7):905–926.
9. Bruneau CHH, Fabrie P, Rasetarinera P. An accurate finite difference scheme for solving convection-dominated diffusion equations. *International Journal for Numerical Methods in Fluids* 1997; **24**:169–183.
10. Tsai T, Yang J, Huang L. An accurate integral-based scheme for advection–diffusion equation. *Communications in Numerical Methods in Engineering* 2001; **17**:701–713.

DOI: 10.1002/fld

11. Deng Z, Singh VP, Bengtsson L. Numerical solution of fractional advection–dispersion equation. *Journal of Hydraulic Engineering* 2004; **130**(5):422–431.
12. Stefanovic DL, Stefan HG. Accurate two-dimensional simulation of advective–diffusive–reactive transport. *Journal of Hydraulic Engineering* 2002; **127**(9):728–737.
13. Leonard BP. A stable and accurate convective modeling procedure based on quadratic upstream interpolation. *Computer Methods in Applied Mechanics and Engineering* 1979; **19**:59–98.
14. Chen Y, Falconer RA. Advection–diffusion modeling using the modified QUICK scheme. *International Journal for Numerical Methods in Fluids* 1992; **15**:1171–1196.
15. Leonard BP, Noye BJ. Second- and third-order two level implicit FDM's for unsteady one-dimensional convection diffusion. *Computational Techniques and Applications*: *CTAC-89*. Hemisphere: New York, 1990; 311–317.
16. Gross ES, Koseff JR, Monismith SG. Evaluation of advective schemes for estuarine salinity simulations. *Journal of Hydraulic Engineering* 1999; **125**(1):32–46.
17. Dehghan M. Crank–Nicolson finite difference method for two-dimensional diffusion with an integral condition. *Applied Mathematics and Computation* 2001; **124**:17–27.
18. Lin P, Man C. A staggered-grid numerical algorithm for the extended Boussinesq equation. *Applied Mathematical Modelling* 2007; **31**:349–368.
19. Wei G, Kirby JT. Time-dependent numerical code for extended Boussinesq equations. *Journal of Waterway*, *Port*, *Coastal*, *and Ocean Engineering* 1995; **121**(5):251–261.
20. Kim J, Moin P. Application of a fractional-step method to incompressible Navier–Stokes equations. *Journal of Computational Physics* 1985; **59**:308–323.
21. Orszag SA. Numerical simulation of incompressible flows within simple boundaries: accuracy. *Journal of Fluid Mechanics* 1971; **49**:75–112.
22. Nassiri M, Babarutsi S. Computation of dye concentration in shallow recirculating flow. *Journal of Hydraulic Engineering* 1997; **123**(9):793–805.
23. Pozrikidis C. *Numerical Computation in Science and Engineering*. Oxford University Press: New York, 1998.
24. Press WH, Flannery BP, Teukolsky SA, Vetterling WT. *Numerical Recipes*. Cambridge University Press: New York, 1992; 569–572.
25. LeVeque RJ. *Numerical Methods for Conservation Laws*. Lectures in Mathematics. Birkhauser: Basel, 1992.
26. Morinishi Y, Lund TS, Vasilyev OV, Moin P. Fully conservative higher order finite difference schemes for incompressible flow. *Journal of Computational Physics* 1998; **143**:90–124.
27. Benton ER, Platzman GW. A table of solutions of the one-dimensional Burgers equation. *Quarterly of Applied Mathematics* 1972; **30**:195–212.
28. Tsai T, Yang J, Huang L. Hybrid finite-difference scheme for solving the dispersion equation. *Journal of Hydraulic Engineering* 2002; **128**(1):78–86.
29. Balzano A. MOSQUITO: an efficient finite-difference scheme for numerical simulation of 2D advection. *International Journal for Numerical Methods in Fluids* 1999; **31**:481–496.
30. Holly Jr FM, Preissmann A. Accurate calculation of transport in two dimensions. *Journal of Hydraulic Engineering* 1977; **103**(11):1259–1277.
31. Simth R, Tang Y. Advection tests of optimal compact implicit scheme. *Journal of Hydraulic Engineering* 2003; **129**(5):408–411.
32. Glass J, Rodi W. A higher order numerical scheme for scalar transport. *Computer Methods in Applied Mechanics and Engineering* 1982; **31**:337–358.
33. Lin B, Falconer RA. Tidal flow and transport modeling using Ultimate Quickest scheme. *Journal of Hydraulic Engineering* 1997; **123**(4):303–314.
34. Wang H, Dahle HK, Espedal MS, Ewing RE, Sharpley RC, Man S. An ELLAM scheme for advection–dispersion equations in two dimensions. *SIAM Journal on Scientific Computing* 1999; **20**(6):2160–2194.

DOI: 10.1002/fld